European Rotorcraft Forum

INVERSE SIMULATION OF A HELICOPTER–TOWING CABLE–SONAR SYSTEM

Giulio Avanzini, giulio.avanzini@unisalento.it, Università del Salento (Italia)
Flavio Liberati, flavioliberati@gmail.com, "Sapienza" Università di Roma, Roma, Italy (Italia)
Guido De Matteis, guido.dematteis@uniroma1.it, "Sapienza" Università di Roma, Roma, Italy (Italia)

Abstract
An inverse simulation algorithm based on an integration method is applied to a system formed by a submerged vehicle towed by a single main rotor helicopter by means of a massive, elastic cable. The problem is split into two phases: at each discretization time-step of the inverse simulation, the trajectory of the cable suspension point is derived first, which results into the submerged vehicle following the desired pattern in water; then the control variables for the helicopter are determined, which make the suspension point follow the trajectory obtained at the previous step, including cable tension as an additional load. The control action is then integrated forward in time for a fully coupled complete helicopter-cable-vehicle system model. Discrepancies in the results between the inverse solution and the forward simulation at the end of the time-step are compensated by (i) introducing a guidance term, which slightly modifies the desired variables at the following step, in order to maintain the towed vehicle on the desired trajectory, and (ii) by an attitude control logic for the helicopter, which manages the variation of moments generated by cable tension. The method is demonstrated for a towed vehicle representative of a realistic sonar system.

1. INTRODUCTION

Environmental monitoring is becoming an increasingly relevant operational scenario in the framework of civil applications of manned and unmanned aerial vehicles. Various sensors can be installed, which provide information for monitoring the conditions of water surfaces, coastlines, air, etc. When scanning possibly wide areas with some sensor or visiting a relevant number of waypoints is required, careful planning of the trajectory results into a more efficient use of vehicles in monitoring tasks. The SAGACE project (*Sistema Avanzato di MonitoraGgio AmbiEntale* in Italian, which translates into *Advanced System for Environmental Monitoring*) is a research program funded by the Apulian Regional Government, aimed at developing innovative low-cost tools for efficient and reliable environmental monitoring, with a particular focus on air and water quality.

Among many others, a set of airborne sensors for air and ground monitoring is being developed by the Department of Mathematics and Physics at the University of Salento and by a small University spin-off company, ISALIT s.r.l., based in Alessandria, Italy. The sensors will be installed on board of multirotor platforms developed by another Italian company, which is a partner in the project, namely IDS S.p.A. At the same time, ISALIT with other partners, such as the Euro-Mediterranean Center on Climate Change (CMCC) and Environmental Surveys S.r.l. (ENSU) are developing a set of techniques for monitoring coastal water. Some of the parameters are measured by means of sensors installed on buoys moored to the seabed, which means that measures are taken in a prescribed and fixed position. In other cases, water is sampled by means of a drone, which retrieves samples of water, to be analyzed in a lab, thus allowing for widening the area of the monitoring action. However, the use of a small unmanned platform significantly limits, at present, the area and the depth that can be reached during a single flight, and it rules out the possibility of real-time results.

Provided that the development of path-planning tools for aerial systems involved in environmental monitoring is one of the objective of the research program, the present paper aims at investigating the possibility of developing such a tool for a helicopter, towing a relatively large submerged vehicle. The vehicle can carry sensors capable of field measurements at different depths, and the cable system provides a direct link to the helicopter for real-time data acquisition and storage. This type of configuration (a rotorcraft towing a submerged load equipped with sensors) is already adopted in mil-

itary application, such as anti-submarine warfare, where a helicopter tows a sonar.[1] A relevant problem in this framework is to evaluate if the mission trajectory envisaged for the submerged sensor platform, determined with respect to monitoring objectives, can be tracked with adequate accuracy. This is done by evaluating the rotorcraft trajectory which results into the desired trajectory of the towed vehicle, checking its feasibility with respect to aeromechanical performance limitations of the helicopter.

The dynamics of rotorcraft with a slung load represents a challenging scenario for helicopter pilots, on the practical operational side, as well as for the flight dynamicists, on the theoretical modeling side. In order to correctly predict dynamic behavior and/or performance limitations, a reliable model capable of correctly capturing the coupled dynamics of vehicle, cable, and load is required, together with suitable analysis tools.[2,3] Piloting and modeling problems become even more severe, when a submerged load is to be dealt with, as in the case of a helicopter towing a submerged load. In such a case[1,4], the cable is partially in the air and partially submerged in water; cable length can become very long (up to values in the order of 10^2 m, in military applications), and, last but not least, a precise trajectory for the towed vehicle may be relevant for the success of the mission.

The objective of this paper is to investigate a method based on inverse simulation (IS)[5,6,7,8] for deriving the control action on the helicopter which results into the sonar following (almost) exactly a prescribed path at an assigned depth, accounting for a reasonably accurate model for each one of the elements of the system, namely the helicopter, the cable, and the submerged load, including all relevant coupling terms. Figure 1 represents a sketch of the problem, where the tension in the cable during the towing task if highlighted. This problem was investigated in previous works[1,4]. In order to allow for a comparison with these studies, reference will be made to the mission analyzed in[1], where (i) the cable is assumed as straight and massless, (ii) the maneuver is decomposed into a set of steady state arcs and segments, and (iii) the resulting trim states are tracked by means of a Linear Quadratic Regulator.

The present work aims at deriving a solution algorithm for the inverse problem, where a massive elastic cable is included in the model, and unsteady maneuver phases are considered within the inverse problem. The elements of the model are

1. the towed submerged vehicle, modeled as a rigid body, featuring a cylindrical fuselage, two low aspect ratio wings and tail appendages (variable wing incidence can be included among system control variables);

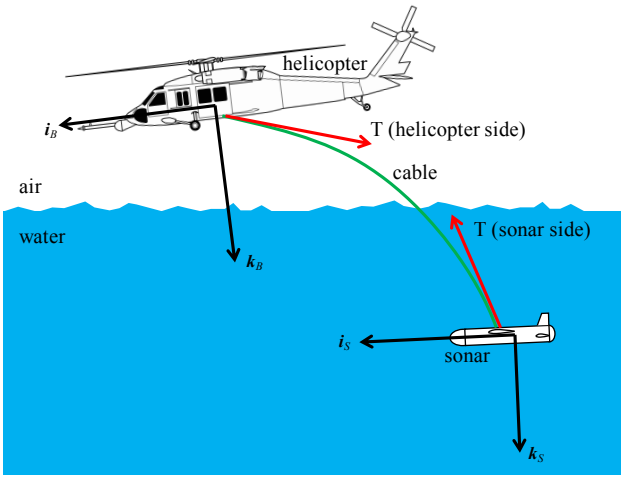

Figure 1: Sketch of the problem.

2. the cable, discretized by means of N elements; where each element is represented by a spring-damper-mass system; aerodynamic or hydrodynamic drag acting on cable elements during motion is included in the model;

3. a medium-complexity helicopter model,[10,11] with rigid fuselage 6 degree-of-freedom dynamics, an aerodynamic model provided by a data-base of force and moment coefficients, individual rigid blade flapping dynamics, three state and single state first-order inflow models for main and tail rotor, respectively.

An integration algorithm is used[6,8], where a piecewise constant control action is determined which results into the prescribed output variables to achieve their desired value at the end of the integration interval. The method is very sensitive to uncontrolled states and non-minimum-phase behavior. One of the contributions of the present work is the determination of a numerically efficient solution strategy for this complex problem, by splitting the inverse simulation problem into two parts.

The towing cable-sonar subsystem is isolated from the helicopter and a nominal inverse problem (IS1) is defined where the trajectory of the suspension point on the helicopter side provides three control variables necessary for making the towed vehicle follow the desired trajectory, where the coordinates of the sonar position as a function of time represent three desired output variables. The resulting trajectory of the suspension point is then used as the tracked output for the inverse problem of helicopter dynamics (IS2), where four control variables are available (namely main rotor collective, longitudinal and lateral cyclic pitch and tail rotor collective pitch) for tracking three desired output variables (the suspension point trajectory). A nominal inverse problem is obtained by enforcing a zero-sideslip constraint. In the framework of IS2, cable

tension, determined during IS1, acts on the suspension point, as an additional load on the helicopter.

Both IS1 and IS2 problems are formulated in terms of velocity variables, that is, sonar velocity and suspension point velocity are used as tracked outputs for IS1 and IS2, respectively. The control action determined by IS2 is used as the input to the fully coupled dynamic model for the forward simulation of the control action determined.

Because of problem discretization, numerical accuracy of the solution, uncoupled helicopter and cable/sonar dynamics in the IS solutions, the assumption of a piecewise constant control action for IS1, and other factors (which will all be discussed in detail in the next sections), the actual trajectory of the sonar during the forward simulation does not track exactly the prescribed one, as defined in the framework of IS1. If no correction is introduced, increasing errors on helicopter and sonar positions builds up, the former being potentially critical as the related cable tension force and moment variations might destabilize the system.

This is avoided by introducing (i) a correction to IS1 tracked output variables, where the desired sonar velocity is augmented by a guidance term, proportional to the position error, following the approach proposed in Ref. 9, for a different framework, and (ii) a simple attitude control functionality, where helicopter Euler's angles are kept close to their reference values generated by IS2. The additional guidance increment of velocity variables was required in Ref. 9 in order to compensate for differences in the models of the same helicopter used in the inverse and forward simulation steps of the IS algorithm. Here the guidance term is required for compensating the errors introduced by coupling the cable-sonar and helicopter models.

In the next section, the rotorcraft-cable-sonar model is presented, together with an analysis of trim states for the whole system. At the beginning of Section 3, general aspects of the inverse simulation algorithm based on an integration method will be recalled, before the details on the formulation of IS1 and IS2 are discussed and a solution method for the coupled problem proposed. Section 4 provides the results of the algorithm. A section of concluding remarks and future activities closes the paper.

2. MODELS AND METHODS

2.1. Rotorcraft model

A medium-complexity helicopter model with articulated rotor blades is adopted, taken from Refs. 10 and 11, representative of a Sikorsky UH-60 "Blackhawk" single main rotor helicopter (Fig. 2). The original model features 6 degrees of freedom for the fuselage, which is assumed rigid. A set of look-up tables provides force and moment aerodynamic coefficients as functions of angle of attack, α, and sideslip angle, β, at hovering and in forward flight. Flap and lag dynamics are considered for each rigid blade, whereas an elastic torsional degree of freedom accounts for blade deformation around the blade pitch axis. Aerodynamic loads on the blade are numerically integrated in the framework of the so-called strip theory, where each airfoil is assumed to develop a local value of lift and drag coefficient per unit blade length, which depends on the local flow angle of attach and Mach number only.

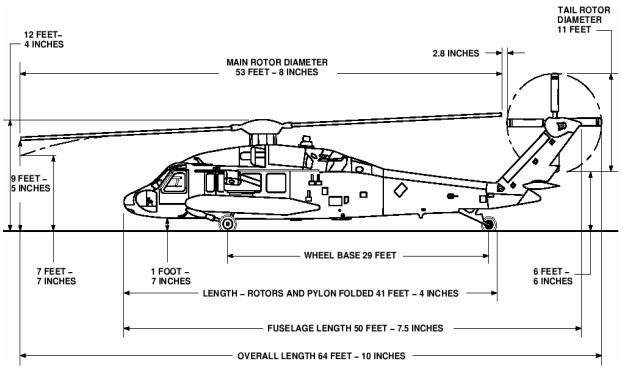

Figure 2: Sikorsky UH-60 "Blackhawk".

A triangular inflow model for the main rotor[12] and a uniform inflow model for the tail rotor complete the aerodynamic model, such that tail rotor inflow velocity is equal to $\nu_{0_{TR}}$, whereas inflow velocity distribution is on the main rotor disk is

$$w_i(\Psi_i, r) = \nu_0 + (\nu_s \sin\Psi + \nu_c \cos\Psi) \cdot (r/R)$$

r being the distance of the airfoil from rotor axis and R blade radius. Blade anomaly for a $N_{bl} = 4$ blade rotor is given by $\Psi_i = \Psi + (i-1) \cdot (\pi/2)$, $i = 1, 2, 3, 4$. Engine dynamics is neglected, and constant main (Ω_{MR}) and tail rotor (Ω_{TR}) angular rates are assumed, with $\dot{\Psi} = \Omega_{MR}$. The original model features a total of 41 state variables. Control variables are represented by main and tail rotor collective pitch, $\theta_{0_{MR}}$ and $\theta_{0_{TR}}$, and main rotor cyclic lateral and longitudinal cyclic pitch, $A_{1,s}$ and $B_{1,s}$.

With respect to the original model, a few modification are introduced. In particular, following the findings discussed in Ref. 13, lag and torsional blade dynamics hardly affect the results of inverse simulation, especially when maneuvers are not aggressive, as it is expected for the present applicative scenario. Hence, helicopter model order is reduced to 25 state variables,

$$\mathbf{x}_H = (\mathbf{x}_{fus}^T, \mathbf{x}_{rot}^T, \mathbf{x}_{inf}^T)^T \in \mathbb{R}^{25}$$

where $\mathbf{x}_{fus} = (\mathbf{v}_B^T, \boldsymbol{\omega}_B^T, \boldsymbol{\Phi}^T, \mathbf{r}_I^T)^T$ are fuselage states, with $\mathbf{v}_B = (u, v, w)^T$ helicopter center of

mass velocity components in the body frame, $\boldsymbol{\omega}_B = (p, q, r)^T$ roll, pitch and yaw angular rates, $\boldsymbol{\Phi} = (\phi, \theta, \psi)^T$ fuselage roll, pitch and yaw angles, $\mathbf{r}_I = (x_I, y_i, z_i = -h)^T$ center of mass position in the inertial frame; rotor states $\mathbf{x}_{rot} = (\dot{\beta}_1, \dot{\beta}_2, \dot{\beta}_3, \dot{\beta}_4, \beta_1, \beta_2, \beta_3, \beta_4, \Psi)^T$ are represented by blade flap rate and angle, $\dot{\beta}_i, \beta_i$, $i = 1, 2, 3, 4$ and reference blade anomaly, Ψ; inflow states are $\mathbf{x}_{inf} = (\nu_0, \nu_s, \nu_c, \nu_{0_{TR}})^T$. Again, the control vector is given by $\mathbf{u}_H = (\theta_{0_{MR}}, A_{1,s}, B_{1,s}, \theta_{0_{TR}})^T \in \mathbb{R}^4$.

2.2. Cable model

The cable is discretized by means of N straight elastic elements and $N + 1$ nodes (Fig. 3), where the position of node 0 is the attach point on the helicopter, whereas node N is the attach point on the submerged vehicle side. A mass $m_i = m_c/(N-1)$ is associated to all the remaining $N - 1$ nodes, where m_c is the total mass of the cable.

Letting $\mathbf{r}_i$ be the position vector of the i-th node, the length of the i-th element is $\ell_i = \|\mathbf{r}_i - \mathbf{r}_{i-1}\|$. The resulting tension in the element, which is the internal force exchanged between nodes i and $i-1$, is given by $T_i = EA\varepsilon_i$, where E is Young's modulus, A the area of the cable section, and $\varepsilon_i = (\ell_i - \ell_0)/\ell_0$, $\ell_0 = L_0/N$ being the length of cable elements at rest (assumed all equal), and L_0 is the length of the whole cable at rest.

Friction between fibers and/or with cable coating dissipates energy. This effect is accounted for by means of a viscous-like damping force, $F_i^d = C_{vd}\dot{\varepsilon}_i$, where the deformation rate in the tangential direction $\hat{\mathbf{q}}_i$ of the i-th element is $\dot{\varepsilon}_i = [(\mathbf{v}_i - \mathbf{v}_{i-1}) \cdot \hat{\mathbf{q}}_i]/\ell_0$. The internal force $\mathbf{f}_i^{int} = (T_i + F_i^d)\hat{\mathbf{q}}_i$ exchanged between each pair of nodes thus lies along $\hat{\mathbf{q}}_i = (\mathbf{r}_i - \mathbf{r}_{i-1})/\|\mathbf{r}_i - \mathbf{r}_{i-1}\|$ and it is equal to that of a spring and a damper in parallel, as represented in the enlarged inset in Fig. 3.

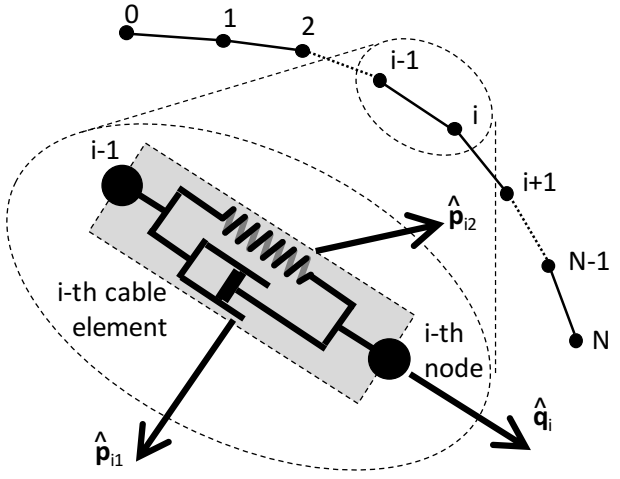

Figure 3: Discretization of the cable.

The derivation of a model for external forces acting on the i-th cable element, equal to the sum of hydrodynamic and buoyancy forces and weight, $\mathbf{f}_i^{ext} = \mathbf{f}_i^h + \mathbf{f}_i^b + \mathbf{f}_i^w$, requires that a set of axis is associated to the element itself. This is done by choosing a local frame $\mathcal{F}_i = \{\hat{\mathbf{q}}_i, \hat{\mathbf{p}}_{i1}, \hat{\mathbf{p}}_{i2}\}$, where $\hat{\mathbf{p}}_{i1}$ is normal to the tangential direction $\hat{\mathbf{q}}_i$, in the vertical plane, and $\hat{\mathbf{p}}_{i2}$ completes a right-handed triad.

Following the approach presented in Ref. 14, and letting $\mathbf{v}_i = (v_{q_i}, v_{p1_i}, v_{p2_i})^T$ be the velocity components of the mid-point of the i-th cable element expressed in $\mathcal{F}_i$, hydrodynamic force exchanged with the surrounding fluid of density ρ_x, is given by $\mathbf{f}_i^h = (f_{q_i}^h, f_{p1_i}^h, f_{p2_i}^h)^T$, with

$$
\begin{aligned}
f_{q_i}^h &= -\text{sign}(v_{q_i})\,\frac{1}{2}\rho_x C_D d_c \ell_0 f_{q_i} \|\mathbf{v}_i\|^2 \\
f_{p1_i}^h &= -\frac{1}{2}\rho_x C_D d_c \ell_0 f_{p_i} \|\mathbf{v}_i\|^2 \frac{v_{p1_i}}{\sqrt{v_{p1_i}^2 + v_{p2_i}^2}} \\
f_{p2_i}^h &= -\frac{1}{2}\rho_x C_D d_c \ell_0 f_{p_i} \|\mathbf{v}_i\|^2 \frac{v_{p2_i}}{\sqrt{v_{p1_i}^2 + v_{p2_i}^2}}
\end{aligned}
$$

where the subscript $x = a$, when the element is in the air and $x = w$, when it is in water, d_c is cable diameter, C_D its drag coefficient, when the flow impinges in a direction normal to $\hat{\mathbf{q}}_i$, and two experimental parameters are introduced,, namely f_{q_i} and f_{p_i}, which depend on the local incidence, η_i (expressed in radians), with

$$
\begin{aligned}
f_{q_i} &= 0.01(2.008 - 0.3858\eta_i + 1.9159\eta_i^2 + \\
&\quad +4.1615\eta_i^3 + 3.5064\eta_i^4 - 1.1873\eta_i^5) \\
f_{p_i} &= 0.5 - 0.1\cos(\eta_i) + 0.1\sin(\eta_i) + \\
&\quad -0.4\cos(2\eta_i)) - 0.11\sin(2\eta_i)
\end{aligned}
$$

Assuming the free surface of water is at $z = 0$, and remembering that altitude $h = -z$, when the usual convention on the direction of the z-axis parallel to the local vertical is adopted, when both nodes $i - 1$ and i are above the surface ($z_{i-1}, z_i < 0$), then air density is assumed, whereas when z_i and z_{i-1} are both positive, both nodes are below the water surface and water density is assumed. Letting k be the index relative to the k-th cable element, such that node k is below the surface ($z_k > 0$) and $k - 1$ above ($z_{k-1} < 0$), drag force is evaluated for both densities and a weighted average is used. Weights are equal to $w_k = z_k/\Delta z_k$ and $w_{k-1} = z_{k-1}/\Delta z_k$, for the k-th and the $(k-1)$-th nodes, respectively, with $\Delta z_k = |z_k - z_{k-1}|$. Other hydrodynamic actions, such as lifting force or added mass effects, are neglected.

Buoyancy and weight both act along the local vertical. Letting $V = A\ell_0$ be the volume of the cable elements, the sum of these two forces is equal

to $\mathbf{f}_i^b + \mathbf{f}_i^w = (\rho_c - \rho_w)V\hat{g}$, where $g = \|\mathbf{g}\|$ is gravity acceleration, directed along the local vertical. Once the total external actions on the i-th cable element are evaluated, it is split in two equal parts and each part is applied, together with tension and internal damping forces, to the massive nodes at the edges of each element. Provided that the mass of all nodes are equal, the resulting equation of motion of the i-th node, $i = 1, 2, \ldots, N-2, N-1$, is thus given in an inertial frame by applying Newton's second law, that is,

$$\begin{aligned} m_i\ddot{\mathbf{r}}_i &= (T_{i+1} + F_{i+1}^d)\hat{\mathbf{q}}_{i+1} - (T_i + F_i^d)\hat{\mathbf{q}}_i + \\ &+ \frac{1}{2}\left(\mathbf{f}_i^h + \mathbf{f}_{i+1}^h\right) + (m_i - \rho_x V)\mathbf{g} \end{aligned} \tag{1}$$

The resulting state vector of the cable model is thus given by $\mathbf{x}_C \in \mathbb{R}^{6(N-1)}$, with

$$\mathbf{x}_C = (\dot{\mathbf{r}}_1^T, \mathbf{r}_1^T; \dot{\mathbf{r}}_2^T, \mathbf{r}_2^T; \ldots; \dot{\mathbf{r}}_i^T, \mathbf{r}_i^T; \ldots; \dot{\mathbf{r}}_{N-1}^T, \mathbf{r}_{N-1}^T)^T$$

2.3. Sonar model

The submerged towed vehicle[1] is made of a 2 m long cylindrical fuselage, with a diameter of 0.25 m. The vehicle features a low-aspect ratio variable-incidence wing, which can be used for controlling vehicle depth, and three fixed tail surfaces, which provide longitudinal and directional restoring moments for static stability and damping moments around the same axes (Fig. 4.a). Relevant dimensions are reported in Fig. 4.b. In what follows, wing incidence will be assumed fixed, in a neutral position. A spherical joint connects the vehicle to the towing cable, which allows all three relative rotational degrees of freedom. Only a tension force is thus exchanged at the joint. Damping around the roll axis is guaranteed by the wing, whereas lateral stability results from the action of the tension force on the joint placed above the center of mass.

The towed vehicle is assumed to be rigid, and a body frame, $\mathcal{F}_L = \{\hat{\mathbf{e}}_{L1}, \hat{\mathbf{e}}_{L2}, \hat{\mathbf{e}}_{L3}\}$ is attached to it, as represented in Fig. 4.a. Its motion is described by a set of 12 nonlinear ordinary differential equations, where all vector quantities with a subscript L are expressed in $\mathcal{F}_L$, given by:

$$\begin{aligned} m_L\left(\dot{\mathbf{v}}_L + \boldsymbol{\omega}_L \times \mathbf{v}_L\right) &= \mathbf{f}_L^h + \mathbf{f}_L^b + m_L\mathbf{g} + \mathbf{t} \\ \mathbf{I}_L\dot{\boldsymbol{\omega}}_L + \boldsymbol{\omega}_L \times (\mathbf{I}_L\boldsymbol{\omega}_L) &= \mathbf{m}_L^h + \mathbf{r}_L^J \times \mathbf{t} \\ \dot{\mathbf{r}}_I^{GL} &= \mathbb{T}_{IL}\mathbf{v}_L \\ \dot{\boldsymbol{\Phi}}_L &= \mathcal{R}^{-1}\boldsymbol{\omega}_L \end{aligned} \tag{2}$$

where $m_L = 450$ kg is the mass of the vehicle, $\mathbf{I}_L = \mathrm{diag}(3.5, 150, 150)$ kg m^2 its inertia tensor, $\mathbf{v}_L = (u_L, v_L, w_L)^T$ the velocity of the center of mass, the position of which in the inertial frame is $\mathbf{r}_I^{GL} = (x_L, y_L, z_L)^T$, $\boldsymbol{\omega}_L = (p_L, q_L, r_L)^T$ its angular velocity, $\mathbf{f}_L^h$ and $\mathbf{m}_L^h$ are hydrodynamic force and moment, $\mathbf{f}_L^b$ and $m_L\mathbf{g}$ are buoyancy force and weight, $\mathbf{t}$ the tension force applied by the cable at the joint, the position of which in $\mathcal{F}_L$ is given by $\mathbf{r}_L^J$. Finally, $\mathbb{T}_{IL}$ is the coordinate transformation matrix from the body to the inertial frame, whereas $\mathcal{R}^{-1}$ relates the angular rates to the evolution of the roll, pitch, and yaw angles, $\boldsymbol{\Phi}_L = (\phi_L, \theta_L, \psi_L)^T$. The state vector of the submerged towed vehicle is thus given by

$$\mathbf{x}_S = (\mathbf{v}_L^T, \boldsymbol{\omega}_L^T, \boldsymbol{\Phi}_L^T, \mathbf{r}_I^{GL\,T})^T \in \mathbb{R}^{12}$$

Only one control variable is present, $\mathbf{u}_L = \theta_w \in \mathbb{R}$, given by the variable incidence of the wing.

In order to evaluate hydrodynamic force and moments, the vehicle is decomposed into 6 elements, namely the fuselage, two half wings, two horizontal tailplanes and one vertical tailplane. Interference and added mass effects are neglected. All hydrodynamic surfaces are characterized by a symmetric airfoil, with a drag coefficient $C_{d_0} = 0.025$ and a lift gradient $C_{\ell_\alpha} = 2\pi$. A parabolic drag polar is assumed, $C_D = C_{D_0} + KC_L^2$, where $K = 1/(\pi \mathcal{A}e)$ (where $\mathcal{A} = b^2/S$ is wing aspect ratio, e its Oswald's factor, b and S wing space and surface, respectively). Neglecting effects at the tip, one has that $C_{D_0} \approx C_d$ and $C_L \approx C_\ell$. A $C_D = 1$ is assumed for the fuselage, with a reference area equal to the section of the cylinder.

The local incidence α_k on the k-th surface can be evaluated from the local velocity with respect to the surrounding water mass, which, for a rigid vehicle, is given by $\mathbf{v}_L^k = \mathbf{v}_L + \boldsymbol{\omega}_L \times \mathbf{r}_L^k$, where $\mathbf{r}_L^k$ is the position vector of the center of pressure of the k-th surface

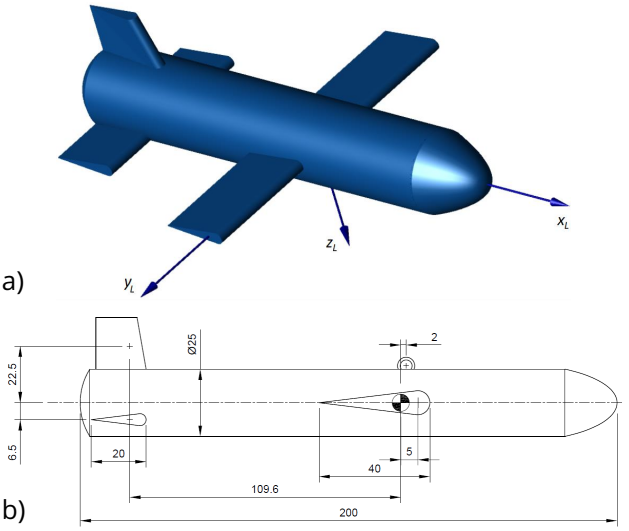

Figure 4: Sketch of the towed vehicle (a) with relevant dimensions in cm (b) (from Ref. [1]).

in $\mathcal{F}_L$. After expressing all the (local) lift and drag components acting on each surface and expressing these hydrodinamic forces in terms of body-frame components, $\mathbf{f}_L^k$, it is possible to write

$$\mathbf{f}_L^h = \sum_k \mathbf{f}_L^k \; ; \;\; \mathbf{m}_L^h = \sum_k \mathbf{r}_L^k \times \mathbf{f}_L^k$$

Finally, buoyancy force and weight, $\mathbf{f}_L^b$ and $m_L\mathbf{g}$, both act along the local vertical, with $\|\mathbf{f}_L^b\| = \rho_w V_L$, V_L being the volume of the vehicle. Gravity is applied to the center of mass, GL. For the sake of simplicity it is assumed that also the buoyancy force is applied to GL, thus neglecting a restoring buoyancy moment, usually negligible with respect to the restoring moment induced by cable tension, $\mathbf{t}$. The latter is equal to the tension in the N-th cable element, applied to the joint in the direction of $\hat{\mathbf{q}}_N$.

2.4. Coupled model and submodels

The state vector of the fully coupled model representing the dynamics of the system is given by

$$\mathbf{x}_S = (\mathbf{x}_H^T, \mathbf{x}_C^T, \mathbf{x}_S^T)^T \in \mathbb{R}^{37+6(N-1)}$$

As for control variables, a fixed neutral 0 deg incidence for the hydrofoil of the towed vehicle wing is assumed, so that no additional control variable is present on the towed vehicle side. The control variables of the complete system thus coincide with those of the helicopter, $\mathbf{u}_S \equiv \mathbf{u}_H \in \mathbb{R}^4$.

Even for relatively small values of the number of cable elements, the order of the system becomes rather large (e.g., for $N = 6$ the order of the system is 67). For this reason, both the trim algorithm, used for mapping cable configuration and vehicle attitude and position at different helicopter forward speed, and the inverse simulation algorithm work on two sub-models. The first one (SM1) consists in the helicopter model, so that its state and control vectors coincide with those listed for the helicopter ($\mathbf{x}_{SM1} \equiv \mathbf{x}_H \in \mathbb{R}^{25}$, $\mathbf{u}_{SM1} \equiv \mathbf{u}_H \in \mathbb{R}^4$). The second sub-model (SM2) is made of the towing cable and the submerged vehicle, so that its state vector is $\mathbf{x}_{SM2} = (\mathbf{x}_C^T, \mathbf{x}_S^T)^T \in \mathbb{R}^{12+6(N-1)}$, without any independent control variable available. The input to this system is represented by position and velocity of the suspension point on the helicopter side, which depend on helicopter motion.

2.5. Trim states

Provided that forces and moments exchanged between rotor blades and helicopter airframe can never be exactly constant in time, a trim state for a rotorcraft is obtained when a set of constant controls $\mathbf{u}_{trim}$ is determined such that state variables are periodic in time, with average values $\bar{\mathbf{x}}$ which provide the desired trim value for airspeed, angular velocity and climb rate.

Trim states for SM1 are obtained by means of a periodic shooting technique,[15] where a periodicity condition is enforced on all state variables, such that $\mathbf{x}(t+T) = \mathbf{x}(t)$, for $T = (2\pi/N_{bl})/\Omega_{MR}$, thus providing, in the present application, 25 periodicity constraints. Four additional trim constraints are also enforced. In the present study, only steady rectilinear flight conditions at zero sideslip are considered as initial conditions for the inverse simulation problem. Letting V_{des} be the desired airspeed, the constraint on average airspeed achieves the form $(\bar{u}^2 + \bar{v}^2 + \bar{w}^2)^{1/2} = V_{des}$, whereas average values of angular and climb rates and sideslip angle are all required to be zero ($\bar{p}^2 + \bar{q}^2 + \bar{r}^2 = 0$, $\bar{\dot{h}} = 0$, and $\bar{v} = 0$). A well posed set of 29 algebraic equations in 29 unknowns (25 state variables at time $t = 0$ and 4 control variables) is obtained, which is solved by means of a Newton-Raphson (NR) method.[16] Trim states of the UH-60 helicopter were analyzed in several works, including Refs. 10 and 11, and are not reported here for the sake of conciseness.

If a straight and level trim condition for the helicopter is dealt with, one can assume that the suspension point on the helicopter side runs along a straight trajectory at constant speed and altitude. This approximation is reasonable, provided that the amplitude of the oscillations of trajectory variables is relatively small. A second trim problem is thus defined for the second sub-system, where all the states of SM2 are required to be constant. In order to reduce the number of unknowns, it is possible to assume that (1) all mass elements of the cable and the towed vehicle moves with the same horizontal velocity, equal to V_{des}; (2) angular rate of the towed vehicle is zero, hence its attitude and course angles are constant. Moreover, assuming a symmetric geometric configuration for the sonar, (3) all the remaining lateral-directional states (namely v_L and ϕ_L) are also 0 and (4) the problem can be reduced to a planar one, where cable and vehicle center of mass all lie on the same plane.

Letting x_0, z_0 be the assigned reference position of the suspension point (with $\dot{x}_0 = V_{des}$), the unknowns of the trim problem for SM2 are represented by a subset of its states, namely

$$\begin{aligned}\hat{\mathbf{x}}_{SM2} \;=\; & (\Delta x_1, z_1, \Delta x_2, z_2, \ldots, \Delta x_i, z_i, \ldots \\ & \ldots, \Delta x_{N-1}, z_{N-1}; \Delta x_{GL}, z_{GL}, \theta_L) \in \mathbb{R}^{3+2(N-1)}\end{aligned}$$

Trim constraints are represented by equilibria for horizontal and vertical force components acting on

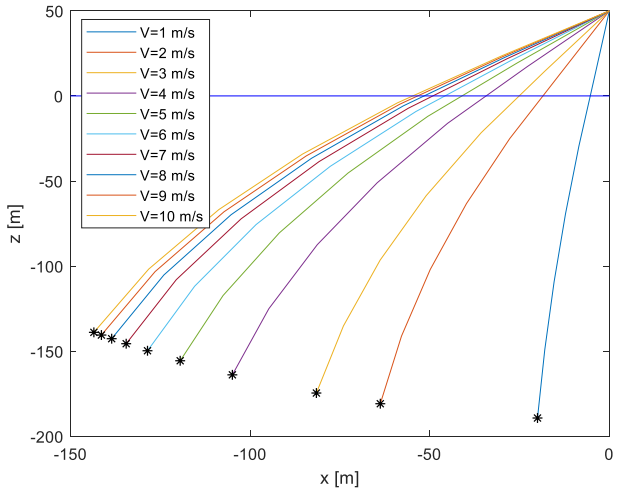

Figure 5: Trim configurations of a 240 m long cable for $1 \leq V_{des} \leq 10$ m/s.

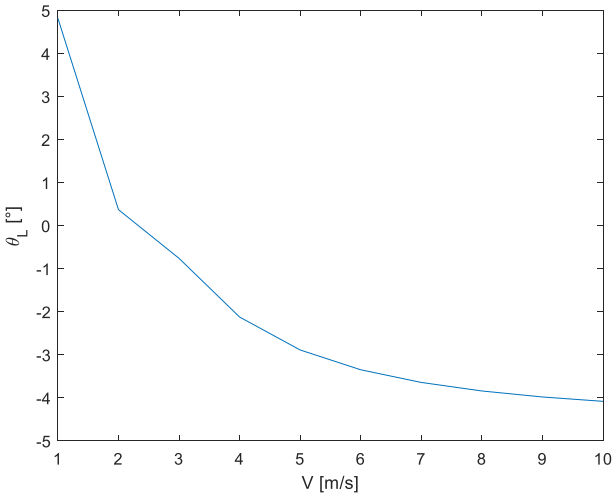

Figure 6: Sonar attitude at trim for $1 \leq V_{des} \leq 10$ m/s.

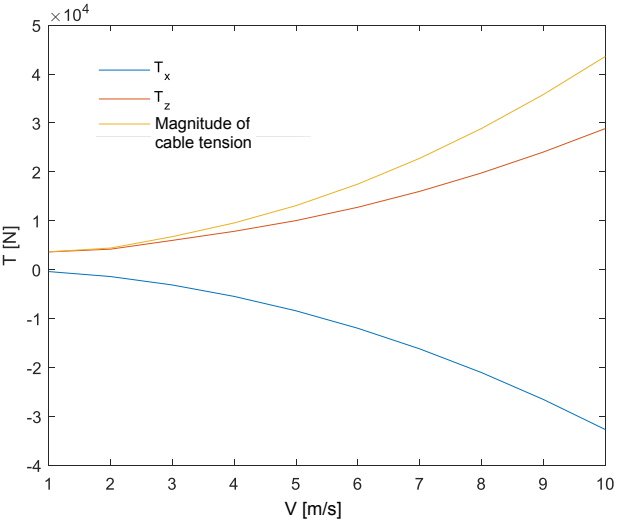

Figure 7: Cable tension (horizontal and vertical components and magnitude) at trim for $1 \leq V_{des} \leq 10$ m/s.

$N-1$ cable mass elements, providing $2(N-1)$ conditions in the form $\ddot{x}_i = \ddot{z}_i = 0$, $i = 1, 2, \ldots, N-1$; longitudinal force and moment equilibria on the towed vehicle provide additional 3 conditions, so that the trim problem for SM2 is also well posed.

The results for the trim problem of SM2 for $N = 6$ are reported in Figs. 5, 6, and 7. With no action on vehicle wing incidence, the position of the vehicle gets closer to the water surface at higher speed, with an increasingly negative displacement in the x direction, due to the increased drag (Fig. 5). Sonar pitch attitude is nose-up at low speed, becoming increasingly negative for $V > 2.5$ m/s (Fig. 6).

Also cable tension steadily increases (Fig. 7), provided it must withstand the vector sum of a (constant) difference between weight and buoyancy (acting along the local vertical) plus steadily increasing drag and lift hydrodynamic force components acting on the towed vehicle (the latter directed downwards, because of the negative pitch attitude at higher speed). Cable tension represents an additional load acting on the helicopter. As a consequence, the trim problem for SM2 needs to be solved first, in order to determine magnitude and direction of tension at the cable suspension point. This force, assumed constant, is applied to the helicopter during the periodic shooting trim of SM1.

An additional constraint on towed vehicle depth can be enforced, if one includes wing incidence θ_w among the unknowns, thus increasing by one the order of the algebraic system to be solved. Trim procedures for SM1 and SM2 during a steady turn are also available. None of these trim problems are addressed here, for the sake of conciseness, provided they play no role in the inverse simulation problem that will be discussed in the next section.

3. INVERSE SIMULATION OF THE ROTORCRAFT-CABLE-SONAR SYSTEM

3.1. Inverse simulation algorithms

Consider a dynamic system, described by a set of ordinary differential equations in the form

$$\dot{\mathbf{x}} = \mathbf{f}(\mathbf{x}, \mathbf{u})$$

with state and control vectors represented by $\mathbf{x} \in \mathbb{R}^n$ and $\mathbf{u} \in \mathbb{R}^m$, respectively. Let

$$\mathbf{y} = \mathbf{g}(\mathbf{x})$$

be a set of tracked output variables, $\mathbf{y} \in \mathbb{R}^p$. An inverse problem is defined when a desired variation of the output variables is prescribed in the time domain, $\mathbf{y} = \mathbf{y}_{des}(t)$, and a control action $\mathbf{u} = \hat{\mathbf{u}}(t)$ is searched for, which produces an evolution of the

state $\hat{\mathbf{x}}(t)$ such that the resulting values of the output variables match the desired ones at all the considered time instants, $\mathbf{g}[\hat{\mathbf{x}}(t)] = \mathbf{y}_{des}(t)$.

When $m = p$, a nominal problem is dealt with, which results into a well posed algebraic problem, when differential methods are adopted.[5] When $m < p$, an underactuated problem is tackled, where the number of available controls does not allow for tracking the prescribed outputs, in the most general case. A minimum error solution can be sought (e.g. in the least square sense), but inverse solution algorithm stability can easily become critical. If $m > p$, a redundant problem is obtained. In this case, while enforcing the required constraints on output variables, it is possible to provide the inverse solution with additional features, relevant for the considered application (e.g. minimum displacements of controls, as in Ref. 8). In what follows, only nominal problems will be dealt with.

Integration methods[6,7,8] are based on the definition of a piecewise constant control action $\mathbf{u}(t) = \hat{\mathbf{u}}_k$ for $t_{k-1} < t \leq t_k$, such that the prescribed constraint is enforced at the end of the considered integration time interval. Assuming the initial state $\mathbf{x}_{k-1}$ at time t_{k-1} is known from the previous time-step, it is possible to numerically integrate system dynamics for a constant value of the control variables, $\hat{\mathbf{u}}_k$, thus deriving $\hat{\mathbf{x}}_k = \mathbf{x}(t_F)$, and the corresponding values of the output variables at time $t_F = t_{k-1} + \Delta T$. The inverse problem is solved when, at convergence, a value of $\hat{\mathbf{u}}_k$ is determined such that the outputs $\mathbf{y} = \mathbf{g}[\hat{\mathbf{x}}(t_F)]$ match their desired values $\mathbf{y}_{des}$ at the same time instant.

Ideally, one would choose $t_F = t_k$, with $\Delta T \equiv \delta t = t_k - t_{k-1}$, adopting a NR solution scheme, for nominal problems, which requires the evaluation of a Jacobian matrix $\mathbf{J}$, the components of which, $J_{i,\ell} = \partial y_i / \partial u_\ell$, need to be numerically determined. The accuracy in the evaluation of $\mathbf{J}$ represents one of the most crucial issues in the definition of the algorithm. In the presence of transmission zeros and/or uncontrolled states $\mathbf{J}$ can become ill-conditioned, causing the inverse simulation algorithm to diverge. This problem is alleviated[8] by integrating the equations of motion for a constant control input over a longer time interval, $\Delta T = N_\tau \delta t$. The control action $\hat{\mathbf{u}}$ which results into the desired outputs to be achieved at time $t_F = t_{k-1} + \Delta T$, is then integrated forward in time between t_{k-1} and $t_k = t_{k-1} + \Delta t$. This allows uncontrolled states to settle, prior to evaluating output variables, at the cost of an increased computational burden, provided all the $p \times m$ simulations required for evaluating $\mathbf{J}$ are performed over a time interval N_τ times longer that δt. Moreover, tracked variables are achieved with a delay.[8]

3.2. Inverse simulation of sonar trajectory

The inverse simulation problem for the cable-sonar system (IS1) consists in the identification of the trajectory of the joint (J) placed at the suspension point of the cable, at the helicopter side, which results into the towed vehicle following (almost) exactly its prescribed pattern. The input variables for the system are velocity components of the suspension point in the inertial frame, $\mathcal{F}_I$. Assuming helicopter altitude is constant, the vertical coordimate of the suspension point is also (at least approximately) constant, hence the corresponding vertical speed component is equal to zero. Only two input variables are thus present, namely $\mathbf{u}_{IS1} = (v_x^J, v_y^J)^T$, which are used for allowing the sonar to track the projection of its prescribed trajectory in the horizontal plane, $\mathbf{y}_{IS1} = (x_I^{GL}(t), y_I^{GL}(t))^T$, thus resulting into a nominal inverse simulation problem, with two tracked variables and two pseudo-control variables.

The integration method is used with an inverse problem discretization interval $\delta t = 0.2$ s and a settling time $\Delta T_1 = 7.0$ s, which corresponds to a value $N_{\tau 1} = 35$. Given the kinematic nature of the problem, it is possible to avoid the use of a (computationally expensive) NR method, circumventing the need for the evaluation of a numerically critical Jacobian matrix of the output variables with respect to pseuto-controls. Letting $\Delta \mathbf{y}_{IS1} = \Delta \mathbf{r}_I^{GL}(t_{F1}) = \mathbf{r}_{L,des}(t_{F1}) - \hat{\mathbf{r}}_I^{GL}(t_{F1})$ (where $\hat{\mathbf{r}}$ is the projection of a position vector $\mathbf{r}$ on the horizontal plane at sonar depth, h_L), a simple iterative scheme is obtained, where

$$\mathbf{u}_{IS1,k}^{(i+1)} = \mathbf{u}_{IS1,k}^{(i)} + \Delta \mathbf{y} / \Delta T_1$$

Convergence is achieved when $\|\Delta \mathbf{y}\| < \varepsilon_r$, with $\varepsilon_r = 0.5$ m. An initial guess is obtained from the solution at convergence for the previous inverse simulation step, $\mathbf{u}_{IS1,k}^{(0)} = \hat{\mathbf{u}}_{IS1,k-1}$.

3.3. Inverse simulation of helicopter motion

Once the trajectory of the cable suspension point is determined from the solution of IS1, the helicopter controls which produce such a trajectory are determined (IS2). This problem is similar to the inverse simulation problem investigated for the same helicopter in Refs. 9 and 13, with the only difference that a trajectory is assigned for a point different from vehicle center of mass. This fact does not increase the difficulty or complexity of the problem, provided that under the assumption of a rigid fuselage, the output variables, represented by the velocity components of the suspension point, are given by

$$\mathbf{y}_{IS2} = \mathbf{v}_I^J = \mathbb{T}_{IB}(\mathbf{v}_B + \boldsymbol{\omega}_B \times \mathbf{r}_B^J) \in \mathbb{R}^3 \quad (3)$$

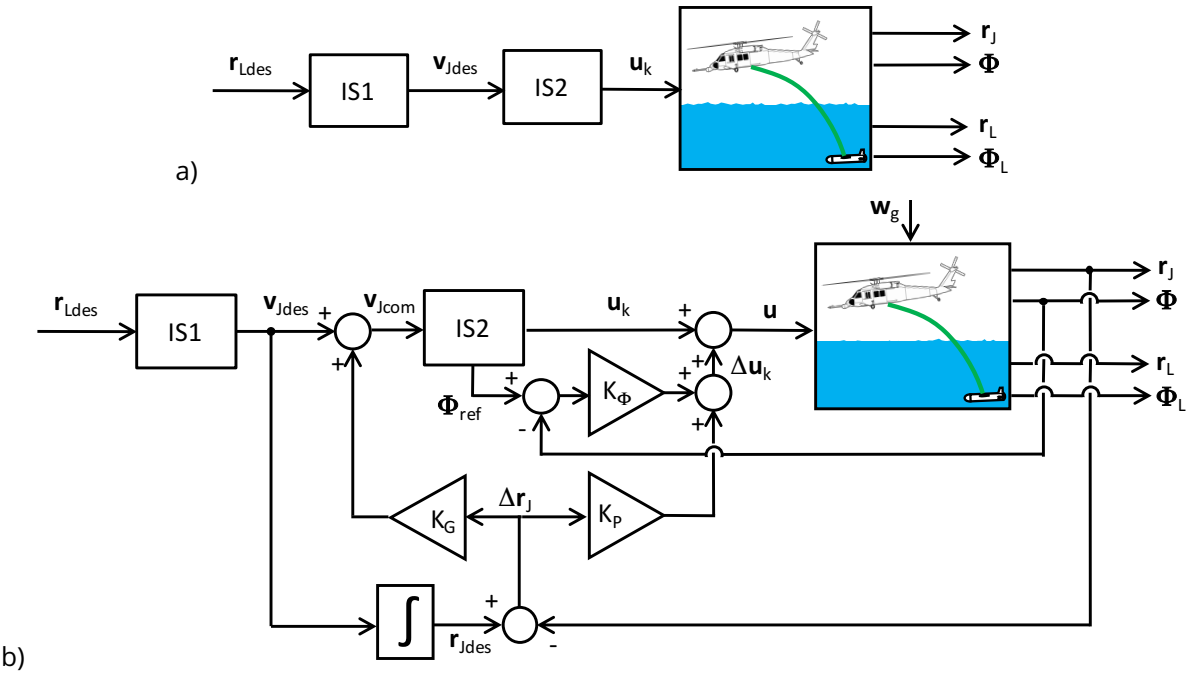

Figure 8: Block diagram of the two-step inverse solution procedure with forward integration of the fully coupled model: (a) simple feedforward of control action to the complete system; (b) scheme with turbulence and compensation of position and attitude errors.

where $\mathbf{r}_B^J = (x_J, 0, z_J)^T$ is assumed to lie on the fuselage longitudinal plane and $\mathbb{T}_{IB}$ is the coordinate transformation matrix from the body to the inertial frame. In the present study, it is $\mathbf{r}_B^J = (0.1, 0, 0.5)^T$ m, so that variations of cable tension produce a significant perturbing pitch moment, which affects helicopter motion.

The desired values of the tracked outputs is given by $\mathbf{y}_{des} = (v_x^J, v_y^J, 0)^T$, where v_x^J and v_y^J are derived from the solution of IS1. A redundant problem is thus formulated for the inverse simulation of helicopter motion, where 4 control variables, $\mathbf{u}_{IS2} \equiv \mathbf{u}_H \in \mathbb{R}^4$ are available for tracking 3 output variables. By requiring that the helicopter flies at 0 sideslip angle, an additional constraint is introduced, transforming IS2 into a nominal inverse problem, where 4 control variables, $\mathbf{u}_H$ are available for enforcing 4 constraints, in the form

$$\mathbf{y}_{IS2} = \mathbf{y}_{des} \; ; \; \beta = 0$$

The same discretization interval used for IS1, $\delta t = 0.2$ s, is adopted also for IS2, in order to easily match the two time-marching procedures. Following the guidelines developed in Refs. 9 and 13, a settling time equal to $\Delta T_2 = 0.6$ s is adopted for IS2, which corresponds to $N_{T2} = 3$, for a numerically more efficient solution, whereas $\Delta T_2 = 1.0$ s is used, if a smoother control action is desired, at the cost of a computational time approximately 40% times longer. More details on the inverse solution of helicopter motion for an articulated blade rotorcraft model by means of integration methods can be found in the cited references.[9,13]

3.4. Inverse solution coupling

The sequence of the solutions for the inverse problems IS1 and IS2 provides an estimate for the control action on the helicopter by solving the inverse problem for sonar trajectory and then finding the control action for the helicopter, which results in the suspension point following the trajectory prescribed by the solution of IS1 over the same time interval. This approach is depicted in the block diagram of Fig. 8.a, where the trajectory of the sonar, $\mathbf{r}_{L,des}$, represents the input to IS1, which determines the velocity components of the cable suspension point on the helicopter side, $\hat{\mathbf{u}}_{IS1} = \mathbf{v}_{des}^J$, which in turn represent the desired outputs tracked by the solution of IS2. This latter inverse problem determines the evolution of helicopter controls $\hat{\mathbf{u}}_k$ which track the variation of $\mathbf{v}_{des}^J$.

Unfortunately, because of the introduction of the settling time ΔT, which causes a delay in the acquisition of the tracked outputs, and other sources of errors in the inverse solutions (problem discretization, convergence accuracy, and so on), discrepancies between the evolution of the output variables for the complete, fully coupled model and their desired values build up during the forward simulation, being initially rather limited, but then becom-

ing possibly relevant. This coupling approach depicted in Fig. 8.a thus can provide just an estimate of helicopter control travel, for a preliminary maneuver feasibility analysis, but not an accurate inverse solution for the fully coupled system, formed by the rotorcraft, the submerged vehicle, and the towing cable connecting them.

For the present applicative scenario, where minor errors in the position of cable suspension point, J, result into sizable variations of tension and even more significant moments applied by the cable to the helicopter fuselage, drift in the error can become severe. The drift can be limited if at each time-step differences between the models at the basis of the inverse solution (two decoupled sub-models) and the model used for the forward simulation (a complete, fully coupled model of the helicopter-cable-sonar system) are accounted for in defining the desired variables and the control action.

A guidance term similar to that adopted in Ref. 9 is introduced. Moreover, a correction to the value of helicopter control variables determined by IS2 is applied, which allows to maintain the prescribed attitude in the presence of errors on the position of the cable suspension point, as depicted in Fig. 8.b. More in detail, at time t_{k-1}, IS1 is solved, thus determining a desired velocity for J, $\mathbf{v}^J_{des} = (v^J_x, v^J_y, 0)^T$, as in the previous case. This signal is integrated forward in time, thus determining also a desired position $\mathbf{r}^J_{des}$ for J, which is compared with the actual position of the suspension point. A velocity command for J is thus provided to IS2, in the form

$$\mathbf{v}^J_{com} = \mathbf{v}^J_{des} + K_G(\mathbf{r}^J_{des} - \mathbf{r}^J_I) \tag{4}$$

where a guidance term is added to the desired velocity obtained from IS1,[9] which compensates for errors in the actual position of J with respect to the desired one. Hence, IS2 is now required to determine a control action on helicopter controls such that $\mathbf{y}_{IS2}$, expressed by Eq. (3), tracks the value of $\mathbf{v}^J_{com}$, expressed by Eq. (4).

Without any further compensation, even a small error on the actual position of the suspension point may generate relevant moments due to cable tension, possibly causing a rapid divergence of rotorcraft attitude motion. For this reason, an attitude control system is introduced, with a simple proportional feedback on Euler's angles, in the form

$$\Delta\mathbf{u}_\Phi = \mathbf{K}_\Phi \Delta\mathbf{\Phi}$$

where $\mathbf{K}_\Phi = \mathrm{diag}(0, k_\phi, k_\theta, k_\psi)$ is control gain matrix and the error signal $\Delta\mathbf{\Phi} = \mathbf{\Phi}_{ref} - \mathbf{\Phi}$ is the difference between a reference value for helicopter Euler's angles during the current time-step, provided by IS2, and the actual value obtained from forward simulation of the complete helicopter-cable-sonar system. When dealing with low-speed, non-aggressive maneuver tasks, as in the present case, control signals around the three axes are decoupled and no increment on collective pitch is included in Euler's angle feedback loop.

The compensation of errors on current attitude is sufficient in the ideal case, when external disturbances are not accounted for. In the presence of wind gusts, as represented by an atmospheric turbulence model, the effect of the difference between groundspeed and airspeed, not accounted for in the framework of the inverse simulation, causes the helicopter to drift away from its prescribed path. A second feedback loop is thus included to maintain the forward simulation close to the specified pattern. This is obtained including another increment to helicopter control in the form

$$\Delta\mathbf{u}_r = \mathbf{K}_r \Delta\mathbf{r}^J$$

where the error signal $\Delta\mathbf{r}^J = \mathbb{T}_{BI}(\mathbf{r}^J_{ref} - \mathbf{r}^J)$, equal to the difference of the desired position of the cable suspension point with respect to its actual position obtained from the forward simulation, projected into a set of body axes, is fed to the collective, lateral and longitudinal cyclic pitch by the gain matrix

$$\mathbf{K}_r = \begin{bmatrix} 0 & 0 & k_h \\ 0 & k_x & 0 \\ k_y & 0 & 0 \\ 0 & 0 & 0 \end{bmatrix}$$

Again, a decoupled set of feedback loops is dealt with for vertical, longitudinal and lateral displacements, a strategy that works well at low speed, below 10 m/s. No feedback to tail rotor collective is present.

4. RESULTS AND DISCUSSION

Various maneuvers have been analyzed, such as 90 deg and 180 deg turns. The latter can be considered as the basic element of a trajectory that scans a given area by means of sensor sweeps along a prescribed direction, where one sweep at constant speed in one direction is followed by a return trajectory displaced by a prescribed amount. As a demanding testbed for the technique, a teardrop trajectory is reported here, for a detailed analysis. The ideal pattern to be followed by the submerged towed vehicle is represented by an initial rectilinear segment approaching the maneuver area, an initial turn to the right, a longer and tighter turn to the left and a final turn to the right which recovers the incoming trajectory in the opposite direction (Fig. 9). The details of the maneuver are reported in Table 1.

Table 1: Relevant parameters for the teardrop trajectory

Constant parameters	**Velocity** V [m/s]	**Altitude** h [m]	**Cable length** L_0 [m]	
(all phases)	10.0	50	240	
Maneuver phase	**Radius** R [m]	**Angular rate** ω [rad/s]	**Angular travel** $\Delta\psi$ [deg]	**Duration** Δt [s]
Approach and exit	—	—	0	20
Turn 1 and 3	300	0.0333	46.97	24.62
Turn 2	140	0.0714	−273.93	66.96

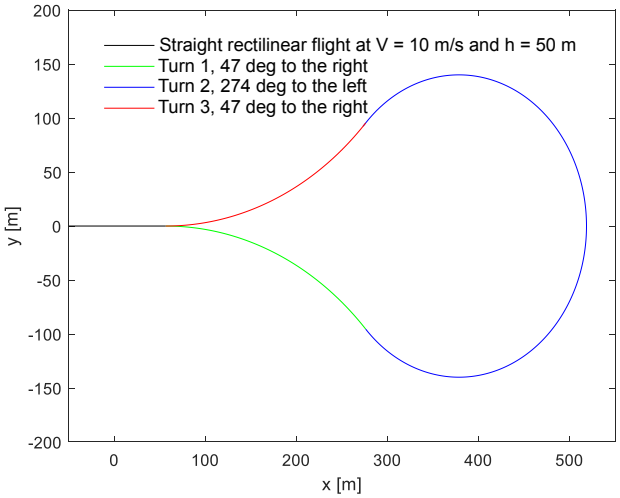

Figure 9: Shape of the teardrop trajectory.

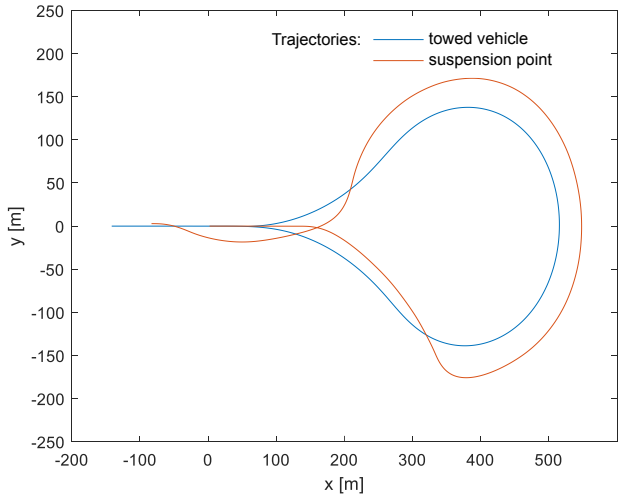

Figure 10: Comparison between the trajectories of the towed vehicle and of the cable suspension point.

The same maneuver was also analyzed in Ref. 1, where a sequence of straight rectilinear and turning steady-state conditions was considered. The inverse simulation approach proposed in this paper fully accounts for maneuver transients, which result into the helicopter following a significantly different pattern, provided that cable dynamic response significantly interfere with how helicopter motion is transferred to the towed vehicle. This is apparent from the solution of IS1, depicted in Fig. 10, where the trajectory of the suspension point is far from being a steady state one, especially in the presence on inflection points, where curvature is reversed.

In the absence of a guidance term for the velocity command, the inverse simulation of helicopter motion (IS2) results in an increasing position error for the suspension point, which ends up to be in the order of a few meters, during the terminal phase of the maneuver. This is clearly unacceptably large, when the control action determined by IS2 is fed to the fully coupled model. The guidance term reduces the error to a fraction of a meter, acceptable, as far as trajectory accuracy is concerned, but still too large, if the forward simulation step is performed not by the decoupled sub-model 2, but using the fully coupled one. Only when a compensation on attitude angle errors is present, which augments the value of helicopter control variables generated by IS2 by means of terms proportional to the errors on roll, pitch, and yaw angles, as discussed in the previous section, the inverse simulation system based on the use of a fully coupled, complete model of the helicopter-cable-sonar system remains stable for the whole duration of the maneuver. The results for tracking performance of towed vehicle and suspension point trajectories are reported in Figs. 11.a and b.

If a turbulence model is included in the forward simulation, in order to simulate realistic environmental conditions, the inverse simulation scheme remains stable, but a drift in the actual positions of helicopter and towed vehicle rapidly builds up. This drift is compensated by introducing a second feedback term, which, as said, augments helicopter controls generated by IS2 by means of a second contribution, proportional to the position error of the helicopter with respect to the desired cable suspen-

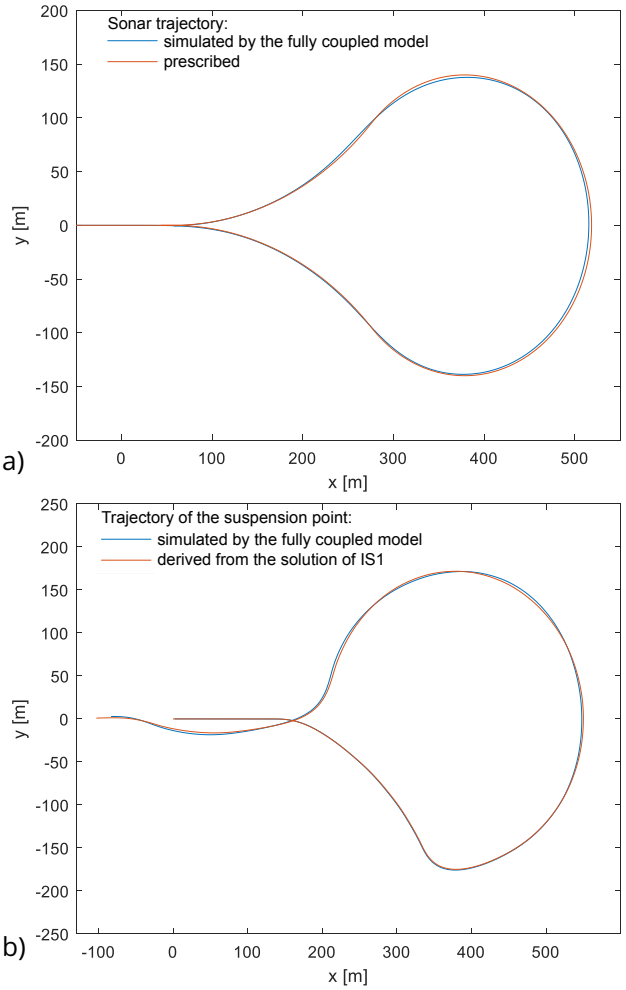

Figure 11: Desired and actual trajectories of the towed vehicle (a) and of the cable suspension point (b) when the forward simulation is performed by means of a complete, fully coupled model of the helicopter-cable-sonar system.

sion point position. The results are almost as good as those presented in Fig. 11, in terms of position accuracy, with a minor increase in position errors and an increased control activity, as visible in Fig. 12. Also the evolution of attitude angles, reported in Fig. 13 for two inverse simulations performed without and with turbulence in the forward simulation step, clearly shows that turbulence induces oscillations on attitude variables that need to be compensated for, in order to maintain the suspension point on the prescribed path.

5. CONCLUSIONS

An inverse simulation algorithm was developed for a system formed by a helicopter towing a submerged vehicle by means of a massive elastic cable. The contributions of the paper lie in the development of an algorithm which accounts for ca-

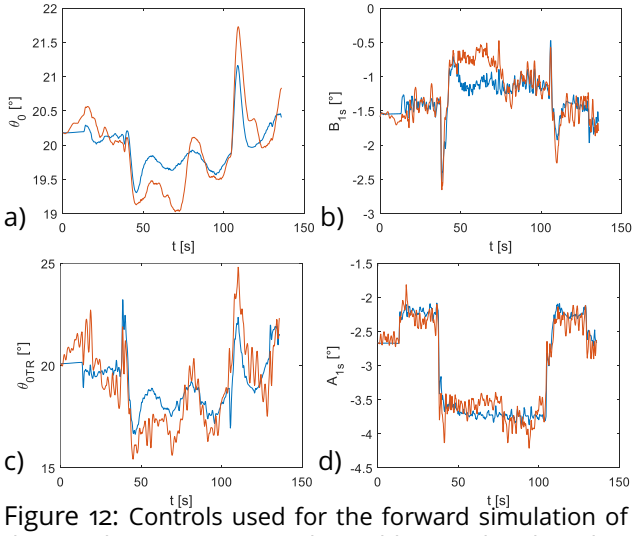

Figure 12: Controls used for the forward simulation of the teardrop trajectory without (blue) and with turbulence (red): collective pitch (a); longitudinal cyclic (b); tail rotor collective (c); lateral cyclic (d).

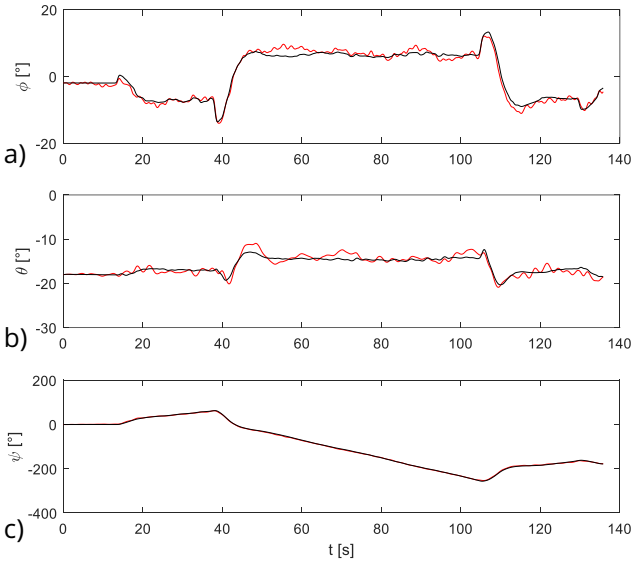

Figure 13: Euler's angles during forward simulation of the teardrop trajectory without (blue) and with turbulence (red): roll (a), pitch (b), and yaw (c) angles.

ble dynamics and maneuver transients, capable of providing a baseline feed-forward control term by means of a two step procedure, based on the solution of two inverse problems. The first inverse problems, for the cable-sonar sub-system, is solved in terms of kinematic variables, where the velocity of the suspension point on the helicopter side is determined, which maintains the center of mass of the towed vehicle on a prescribed path. The second inverse problem allows one to determine the evolution of helicopter controls which make the suspension point follow the pattern determined during the first step. When a fully coupled model is adopted in forward simulation, the use of simple proportional

feedback on attitude and position variables allows to maintain algorithm stability, and adequate tracking performance also in the presence of a simulation of atmospheric turbulence.

ACKNOWLEDGMENTS

The research was supported by the European Union and the Apulian Local Government through the call Innonetwork (POR Puglia FESR - FSE 2014-2020, European Fund for Regional Development, Action 1.6), project SAGAcE (Advanced System for Environmental Monitoring), project number M7X3HL2. The first author would like to thank Marianovella Mello, for her contribution as Project Manager.

REFERENCES

[1] Sridharan A., Simulation Modeling of Flight Dynamics, Control and Trajectory Optimization of Rotorcraft Towing Submerged Loads, Ph.D. Thesis, University of Maryland, 2014.

[2] Williams P., Sgarioto D., Trivailo P., Optimal Control of an Aircraft-Towed Flexible Cable System. J. of Guidance, Control, and Dynamics, 2006, 29(2).

[3] Bisgaard M., Modeling, Estimation, and Control of Helicopter Slung Load System, Ph.D. Thesis, Aalborg University, 2008.

[4] Xin H., He C., High Fidelity Simulation Model for Comprehensive Analysis of Rotorcraft Towing Operations, 59th American Helicopter Society Annual Forum 2003, 6-8 May 2003, Phoenix (AZ), USA.

[5] Kato O., Sugiura I. , "An Interpretation of Airplane General Motion and Control as Inverse Problem," *Journal of Guidance, Control, and Dynamics*, Vol. 9, No. 2, March-April 1986, pp. 198-204. doi:10.2514/3.20090

[6] Hess R. A., Gao C., Wang S. H., "Generalized Technique for Inverse Simulation Applied to Aircraft Maneuvers," *Journal of Guidance, Control, and Dynamics*, Vol. 14, No. 5, Sept.-Oct. 1991, pp. 920-926. doi:10.2514/3.20732

[7] Hess R. A., Gao C., "A Generalized Algorithm for Inverse Simulation Applied to Helicopter Maneuvering Flight," Journal of the American Helicopter Society, Vol. 38, No. 4, Oct. 1993, pp. 3-15. doi:10.4050/JAHS.38.3.

[8] De Matteis G., De Socio L. M., Leonessa, A., "Solution of Aircraft Inverse Problems by Local Optimization," Journal of Guidance, Control, and Dynamics, Vol. 18, No. 3, May-June 1995, pp. 567-571. doi:10.2514/3.21424

[9] Torasso A., Avanzini G., Thomson D.G. "Model Predictive Control Scheme for Rotorcraft Inverse Simulation," Journal of Guidance Control and Dynamics, Vol. 36, No. 1, doi: 10.2514/6.2011-6634.

[10] Howlett J. J., "UH-60A 'Black Hawk' Engineering Simulation Program, Volume 1: Mathematical Model," NASA CR 166309, 1981.

[11] Howlett J. J., "UH-60A 'Black Hawk' Engineering Simulation Program, Volume 2: Background Report,"NASA CR 166310, 1981.

[12] Peters D. A., Ha Quang N., "Dynamic Inflow for Practical Applications," Journal of the American Helicopter Society, Vol. 33, No. 4, Oct. 1988, pp. 64-68. doi:10.4050/JAHS.33.64

[13] Avanzini G, De Matteis G., Torasso A, "Assessment of Helicopter Model Accuracy Through Inverse Simulation," Journal of Aircraft, Vol. 54, No. 2, July 2016, pp. 1-13; doi: 10.2514/1.C033847

[14] Buckham B.J., Dynamics Modelling of Low-Tension Tethers for Submerged Remotely Operated Vehicles, Ph.D. Thesis, University of Victoria, 2003.

[15] McVicar J., Bradley R., "Robust and Efficient Trimming Algorithm for Application to Advanced Mathematical Models of Rotorcraft," Journal of Aircraft, Vol. 32, No. 2, 1995, pp. 439-442.

[16] Press W.H., Teukolsky S.A., Vetterling W.T., Flannery B.P. *Numerical Recipes. The Art of Scientific Computing*. 3rd Edition, Cambridge University Press, New York, 2007, Chapter 9.